Journal of Biosciences and Medicines, 2026, 14(4), 169-183
https://www.scirp.org/journal/jbm
ISSN Online: 2327-509X
ISSN Print: 2327-5081

Study on the Effects of *Erythropalum scandens* Bl. Polysaccharides in Improving Glucose Metabolism Disorder in HUA Rats

Liyang Zhao[1], Qiaodan Pan[1,2*], Yuanhe Hang[1,2], Lingying Zhu[1]

[1]Youjiang Medical University for Nationalities, Baise, China
[2]Key Laboratory of Research on Characteristic Ethnic Medicines in Youjiang River Basin, Colleges and Universities of Guangxi, Baise, China
Email: *panqao112@ymun.edu.cn

How to cite this paper: Zhao, L.Y., Pan, Q.D., Hang, Y.H. and Zhu, L.Y. (2026) Study on the Effects of *Erythropalum scandens* Bl. Polysaccharides in Improving Glucose Metabolism Disorder in HUA Rats. *Journal of Biosciences and Medicines*, **14**, 169-183.
https://doi.org/10.4236/jbm.2026.144014

Received: March 10, 2026
Accepted: April 12, 2026
Published: April 15, 2026

Abstract

Objective: To investigate the extraction process of *Erythropalum scandens* Bl. polysaccharides (ESP) and its ameliorative effect on glucose metabolism in rats with hyperuricemia (HUA). **Methods:** ESP was extracted from *Erythropalum scandens* Bl. using hot water extraction combined with ethanol precipitation. The polysaccharide content was determined via the phenol-sulfuric acid method, and the protein content was measured using the Coomassie brilliant blue method; the yield of crude polysaccharide was employed as the core evaluation index. For *in vivo* animal experiments, a rat model of HUA complicated by glucose metabolism disorders was established in Sprague-Dawley (SD) rats by feeding a fructose-rich and high-fat diet combined with intraperitoneal injection of potassium oxonate (OXO, 200 mg/kg/d). Forty specific pathogen-free (SPF) male SD rats were randomly divided into four groups: the Control group, Model group, ESP low-dose group (ESP-L group), and ESP high-dose group (ESP-H group). Following successful model establishment, the rats were administered the corresponding interventions for 4 weeks. Serum levels of fasting blood glucose (FBG) and uric acid (UA) were detected, and pathological changes in the liver, kidney, and pancreatic tissues were observed by hematoxylin-eosin (HE) staining. **Results**: The phenol-sulfuric acid method demonstrated that the polysaccharide content of crude ESP was 51.73%, with a protein removal rate of 80.83%. Compared with the Model group, ESP significantly reduced serum UA and FBG levels in rats, with a more pronounced effect observed in the ESP-H group. Histopathological findings indicated that ESP alleviated hepatic steatosis and mitigated damage and dysfunction of renal glomeruli, renal tubules, and pancreatic islet β-cells. **Conclusion**: ESP can promote glucose transport and enhance urate transport capacity,

thereby ameliorating glucose and uric acid metabolic disorders in fructose-induced HUA rats. This study provides experimental evidence to support the development of ESP as an interventional agent for metabolic diseases.

Keywords

Erythropalum scandens Bl. Polysaccharides, Hyperuricemia, Glucose Metabolism Disorder

1. Introduction

Metabolic syndrome (MetS) constitutes a major global public health challenge. Notably, the comorbidity rate of hyperuricemia (HUA) and type 2 diabetes mellitus (T2DM) has been on the rise annually. According to 2023 data from the International Diabetes Federation (IDF), 30% - 50% of patients with T2DM worldwide also suffer from HUA, which significantly elevates the risk of diabetic nephropathy, non-alcoholic fatty liver disease (NAFLD), and cardiovascular complications [1]. Clinical studies have demonstrated that excessive fructose intake is a critical trigger for the co-occurrence of HUA and T2DM, and is also a key intervention used to establish metabolic disorder models in laboratory settings [2].

Hyperuricemia is frequently accompanied by diabetes and hyperlipidemia, forming a "triad of metabolic disorders". A major contributing factor to this triad is long-term high fructose consumption, while a high-fat diet further exacerbates oxidative stress and chronic inflammation, thereby disrupting glucose and lipid homeostasis [3]. The unique metabolic characteristics of fructose underlie its multiple disruptive effects on glucose and uric acid metabolism. In the liver, fructose is exclusively phosphorylated by ketohexokinase (KHK) to form fructose-1-phosphate in an insulin-independent manner. This process rapidly depletes adenosine triphosphate (ATP) and generates adenosine monophosphate (AMP), which is further catabolized to inosine monophosphate (IMP) and ultimately to uric acid, directly elevating serum uric acid levels [4]. Meanwhile, AMP depletion impairs the activity of AMP-activated protein kinase (AMPK), a key cellular energy sensor. Reduced AMPK activity activates sterol regulatory element-binding protein-1c (SREBP-1c), which in turn upregulates the expression of fatty acid synthase (FAS) and acetyl-CoA carboxylase 1 (ACC1). This sequence of events promotes hepatic lipogenesis, leading to hypertriglyceridemia and non-alcoholic fatty liver disease (NAFLD) [5]. Additionally, AMPK inhibition decreases the membrane localization of glucose transporters 4 and 2 (GLUT4/GLUT2), reducing glucose uptake in peripheral tissues; it also upregulates glucose-6-phosphatase (G6PC) to enhance gluconeogenesis. These two effects collectively exacerbate hyperglycemia and insulin resistance [6]. Currently, clinical treatments for metabolic syndrome mostly target a single pathway and lack comprehensive strategies to simultaneously regulate glucose and uric acid metabolism.

Erythropalum scandens Bl. is a liana species belonging to the family Olacaceae, primarily distributed in southern China. In traditional Chinese medicine (TCM), it is commonly used to clear heat, promote diuresis, eliminate toxins, and reduce swelling, and is clinically prescribed for the treatment of damp-heat jaundice, rheumatic arthralgia, and other related conditions. Polysaccharides isolated from its stems, designated as ESP, have been shown to exert distinct anti-inflammatory and antioxidant activities.

Previous studies have confirmed that ESP promotes the expression of uric acid transporters, including URAT1 and OAT3, thereby accelerating uric acid excretion. However, the systemic regulatory effects of ESP on metabolism in rats with HUA complicated by glucose metabolism disorders remain unclear. In the present study, we purified ESP and employed serum biochemical analysis and histopathological examination to explore its interventional effects on rats with hyperuricemia and glucose metabolism disorders. The findings of this study are expected to provide experimental evidence to support the clinical application of ESP.

2. Materials

2.1. Raw Materials

Erythropalum scandens Bl. was provided by Guangxi *Erythropalum scandens* Biotechnology Co., Ltd.

2.2. Main Reagents and Instruments

Fructose and potassium oxonate were purchased from Shanghai Adamas Reagent Co., Ltd.; 60% high-fat diet was obtained from Hunan Syno Biological Technology Co., Ltd.; ESP was prepared in the laboratory; Urethane was supplied by Shanghai Hengyuan Biotechnology Co., Ltd.; Detection kits for serum FBG and UA were purchased from Suzhou Grace Bio-Technology Co., Ltd.; Blood glucose meter (Sinocare EA-19) was purchased from Sinocare Inc.; Tissue clearing and deparaffinizing agent as well as alcoholic Eosin Y staining solution were obtained from Zhuhai Baso Biotechnology Co., Ltd.; Hematoxylin bluing solution was purchased from Wuhan Servicebio Biotechnology Co., Ltd. The Motic BA210 digital biological microscope and Motic BA600 virtual slide scanning system, used for the histological analysis of liver, kidney and pancreatic tissues, were both provided by Motic China Group Co., Ltd. (Xiamen, China). The LB941 multifunctional microplate reader (Berthold Technologies GmbH & Co. KG, Germany) was purchased from Hunan Xiangyi Laboratory Instrument Development Co., Ltd. The B-100 rotary evaporator was a product of BUCHI Labortechnik AG (Switzerland). The FA1204B electronic analytical balance was manufactured by Shanghai Techcomp Precision Instruments Co., Ltd. Both the SHB-III circulating water multipurpose vacuum pump and DLSB-5/10 low-temperature cooling liquid circulation pump were products of Zhengzhou Greatwall Scientific Industrial and Trade Co., Ltd.

2.3. Experimental Animals

Forty SPF-grade male Sprague-Dawley (SD) rats, aged 6 - 8 weeks, were purchased from Guangdong Weitong Lihua Experimental Animal Technology Co., Ltd. and raised in the Animal Experiment Center of Youjiang Medical University for Nationalities. The animal production license number was SCXK (Yue) 2022-0063, and the experimental animal use license number was SYXK (Gui) 2022-0004. The rats were housed under the controlled conditions of constant temperature (24˚C ± 2˚C) and relative humidity (50% - 70%), which complied with the requirements for medical experimental animal facilities. The basal diet was the special feed for experimental animals. The ethical review number of the animal experiment was 2024102501.

3. Experimental Methods

3.1. Extraction Process of ESP

1 - 2 kg of *Erythropalum scandens* Bl. powder was weighed and mixed with 95% ethanol at a solid-liquid ratio of 1:20 (g/mL). Reflux extraction was performed once at 70˚C for 1 hour to remove pigments and lipids. The mixture was suction-filtered, and the residue was dried for subsequent use. The treated residue was mixed with ultrapure water at a solid-liquid ratio of 1:20 (g/mL) and soaked for 2 hours, followed by extraction twice at 80˚C for 1 hour each time. The extract was filtered, and the filtrate was subjected to reflux evaporation and concentrated to 1/4 of its original volume. Alcohol precipitation was then conducted by adding anhydrous ethanol to the concentrated solution to adjust the anhydrous ethanol concentration to 50%. After thorough stirring, the mixture was statically placed at a low temperature (4˚C) overnight, then centrifuged at 3000 r/min for 20 minutes. The precipitate was collected and freeze-dried to obtain crude polysaccharides. The crude polysaccharides were dissolved in a small amount of water and subjected to decolorization and deproteinization using a macroporous adsorption resin, with 50% ethanol as the eluent. The eluates were collected, combined, concentrated and freeze-dried for subsequent use.

3.1.1. ESP Content Determination Method

Glucose was used as the standard solution. Precisely weigh 10 mg of anhydrous dried glucose, dissolve it in pure water and dilute to the mark in a 10 mL volumetric flask, and shake well to obtain a 1 mg/mL glucose standard stock solution. For standard curve preparation, the glucose standard solution was diluted into five concentration gradients (0.1, 0.2, 0.3, 0.4 and 0.5 mg/mL), with three parallel experiments set up and each determination repeated three times per group. The detailed operation steps were as follows: pipette each gradient solution into 5 mL stoppered test tubes, add phenol reagent and cap the test tubes, then slowly add concentrated sulfuric acid along the tube wall and shake well. The mixture was placed at room temperature for 30 minutes, then heated in a constant temperature water bath at 90˚C for 15 minutes and cooled to room temperature. Using ul-

trapure water as the blank control, the absorbance value at 490 nm (A_{490nm}) was measured with a microplate reader. The glucose concentration was set as the X-axis and the absorbance value as the Y-axis to plot the standard curve.

$$\text{Polysaccharide content (\%)} = [(C \times D \times V)/(m \times 10^3)] \times 100\%$$

where: C = glucose concentration in the sample assay solution obtained from the standard curve after blank correction (mg/mL); V = total volume of the sample extract after constant volume (mL); D = dilution multiple before determination; m = initial sample weight (g); 10^3 = unit conversion factor (converting mg to g for consistency with the unit of initial sample weight).

3.1.2. Determination of ESP Protein Content

After the crude polysaccharides were deproteinized by macroporous adsorption resin, the Coomassie Brilliant Blue method was used to determine the protein content. The detailed operation was as follows: prepare bovine serum albumin (BSA) standard solutions with five concentration gradients (0.1, 0.2, 0.3, 0.4 and 0.5 mg/mL). Pipette each standard solution into glass test tubes, add Coomassie Brilliant Blue solution to each tube and dilute to the mark, mix thoroughly and let stand at room temperature for 5 minutes. The absorbance value was measured at 595 nm within 20 minutes. The absorbance value was set as the ordinate and the BSA content (mg) as the abscissa to plot the protein standard curve. An aliquot of the crude polysaccharide solution was also treated and assayed according to the above steps and conditions, and its absorbance value at 595 nm was measured and substituted into the standard curve to calculate the protein content in the crude polysaccharides.

$$\text{Protein removal rate (\%)} = [(m_{\text{Before deproteinization}} - m_{\text{After deproteinization}})/m_{\text{Before deproteinization}}] \times 100\%$$

3.2. Rat Feeding and Establishment of Hyperuricemia (HUA) Rat Model with Glucose Metabolism Disorder

A total of 40 male Sprague-Dawley (SD) rats aged 6 - 8 weeks were housed in separate cages based on their body weight and acclimatized for one week; the housing environment was maintained under a 12 h light/12 h dark cycle, with free access to food and water, and the rats were fed with standard SPF-grade basal feed. After one week of acclimatization, the rats were rehoused for model establishment. The grouping was as follows: the Control group was fed with a basal diet; the Model group was fed with a high-fat diet, provided with drinking water containing 30% - 40% fructose ad libitum, and intraperitoneally injected with potassium oxonate daily for 20 weeks; the ESP-administered groups included the ESP high-dose (ESP-H, 3 g/kg/d) and ESP low-dose (ESP-L, 3 g/kg/d) groups, which were given intragastric gavage for 4 weeks. For model establishment, 30 rats were gradually fed with SPF-grade high-fat feed; their body weight was measured weekly, and fasting blood glucose was detected in the morning after 12 hours of fasting. The remaining 10 rats served as the blank Control group, which continued to be fed with SPF-grade basal feed, and changes in their body weight and blood

glucose were recorded simultaneously. During the modeling period, blood glucose was measured by tail-tip blood sampling; combined with the rats' body weight, dietary intake, and general physical condition, rats with blood glucose levels close to 11.1 mmol/L that remained stable for approximately two weeks were selected as ideal hyperuricemia (HUA) rat models with glucose metabolism disorders. These rats were then regrouped according to their blood glucose levels to ensure the randomness and scientificity of grouping, with 10 rats in each group. At the end of the 4-week administration period, all rats were sacrificed, and samples were collected for subsequent experiments.

3.3. Staining of Tissue Sections

Liver, pancreas, and kidney tissues were harvested and cut into 1 cm × 1 cm square pieces, which were then placed into embedding cassettes. After fixation in 4% paraformaldehyde for 24 hours, the tissues were subjected to dehydration, paraffin embedding, sectioning (4 μm), hematoxylin-eosin (HE) staining, and mounting. The morphological changes of the tissues were observed under a light microscope.

The NAFLD Activity Score (NAS) was independently evaluated in a blinded manner by two experienced pathologists. For each group, five liver tissue sections were randomly selected. Each section was systematically observed in 10 fields at 400× magnification. Three parameters were assessed in each field: steatosis, hepatocyte ballooning, and lobular inflammation.

Each parameter was scored based on the percentage of the affected area using a 4-point scale as follows:

- Score 0: No steatosis, no hepatocyte ballooning, and no lobular inflammation;
- Score 1: Mild steatosis (5% - 33%), a small number of ballooned cells, and 1 - 2 foci of necrosis;
- Score 2: Moderate steatosis (34% - 66%), numerous ballooned cells, and 2 - 4 foci of necrosis;
- Score 3: Severe steatosis (>66%), no ballooning, and >4 foci of necrosis.

The total score for each field was the sum of the scores from the three parameters.

3.4. Data Analysis

Statistical analysis was conducted using IBM SPSS Statistics 26 software. Quantitative data were expressed as mean ± standard deviation ($\overline{x} \pm s$). One-way analysis of variance (ANOVA) was used to compare the differences among multiple groups, with a P-value < 0.05 considered statistically significant. GraphPad Prism 8 and Origin software were employed for the construction of experimental figures and tables.

4. Results

4.1. Determination of ESP Content and Protein Content

In this study, the crude extract yield of ESP obtained from 500 g of *Erythropalum*

scandens Bl. was 3.189 g; as shown in Figure 1(A), regression analysis was performed using the least squares method, and the glucose standard curve equation was obtained as: $y_1 = 1.0459x_1 + 0.0445$, $R^2 = 0.9952$; where x_1 represents concentration (mg/mL) and y_1 represents absorbance. As shown in Figure 1(B), the protein standard curve was: $y_2 = 1.441x_2 + 0.0747$, $R^2 = 0.9912$; where x_2 represents concentration (mg/mL) and y_2 represents absorbance. According to the formula, the protein removal rate reached 80.83%. These results demonstrated that after deproteinization by macroporous adsorption resin, the protein content in the polysaccharide sample was significantly reduced, which effectively improved the purity, enhanced the biological activity and stability of ESP, and laid a solid foundation for the subsequent experiments.

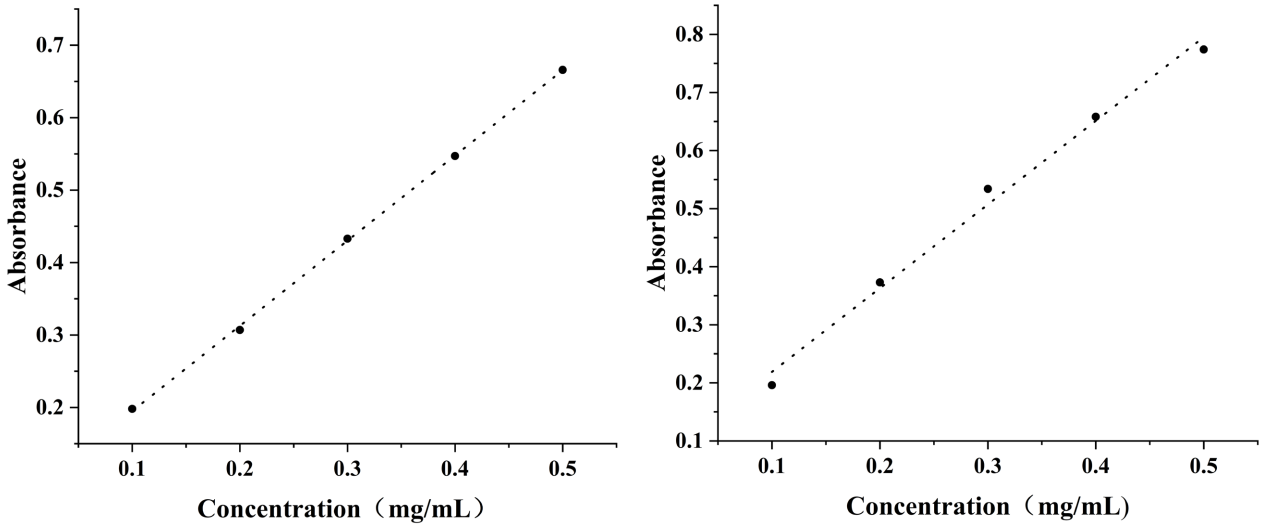

Note: Panel A shows the standard curve of glucose; Panel B shows the standard curve of protein.

Figure 1. Determination of *Erythropalum scandens* Bl. Polysaccharides.

4.2. ESP Improves Body Weight and Blood Glucose Indexes in HUA Rats

4.2.1. Body Weight of Rats

Glucose and lipid metabolism disorders induced by diabetes are core pathological features of metabolic diseases. Rats induced by a high-sugar and high-fat diet exhibited a significant increase in body weight accompanied by abdominal obesity at the initial stage of modeling, which was closely related to increased fat synthesis and imbalanced energy metabolism caused by decreased insulin sensitivity. During the experiment, the body weight of rats in the Model group was significantly higher than that in the Control group (as shown in Figure 2). After 4 weeks of intervention, compared with the Model group, diabetic symptoms in the ESP-H and ESP-L groups were alleviated, and body weight was decreased with an obvious recovery trend, indicating that ESP exerts an improving effect on glucose metabolism.

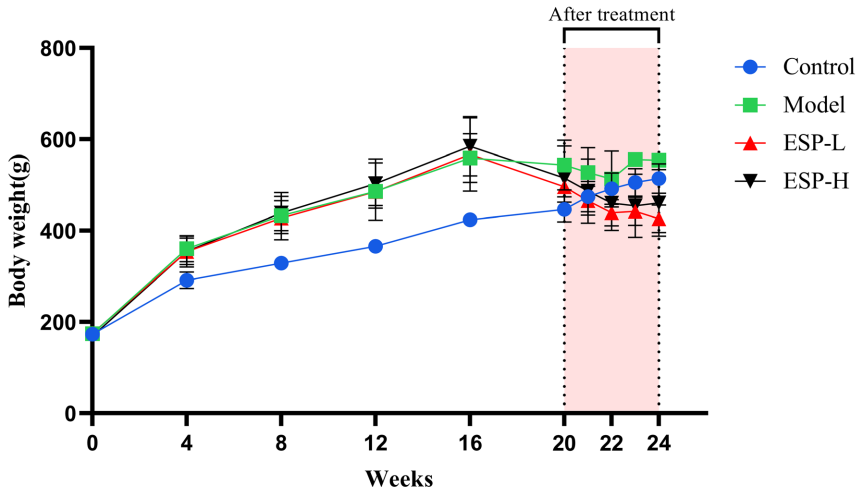

Note: Figure 2 records the body weight of rats during modeling and treatment.

Figure 2. Body weight of rats.

4.2.2. ESP Improves Blood Glucose Indexes in HUA Rats

To validate the successful establishment of a glucose metabolism disorder model in HUA rats, this study evaluated key blood glucose parameters. As shown in Figure 3(A), rats subjected to high-fat diet combined with fructose and OXO administration exhibited significantly elevated blood glucose concentrations compared to the Control group ($P < 0.0001$), confirming successful model induction. Further pharmacodynamic analysis, Figure 3(B) revealed that following 4 weeks of continuous intervention with high- and low-dose ESP (ESP-H and ESP-L), fasting blood glucose levels showed a significant decreasing trend relative to the Model group ($P < 0.05$).

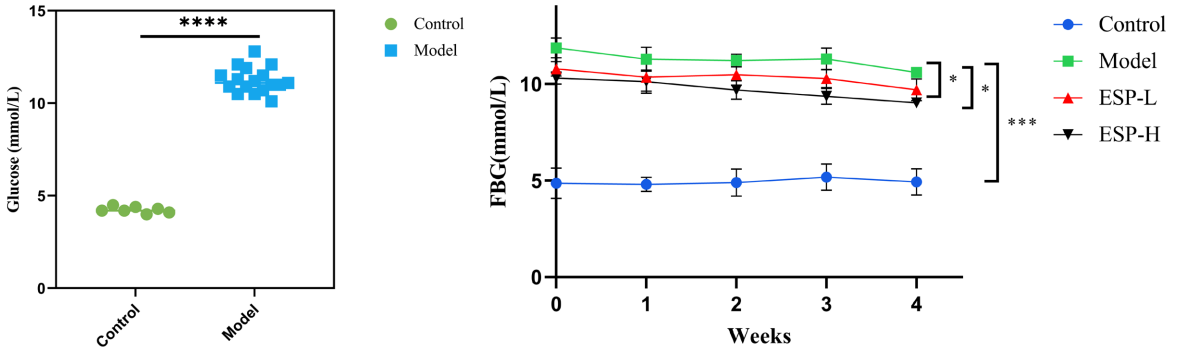

(A) (B)

Note: Panel A shows the blood glucose levels in the Control and Model groups; Panel B shows the fasting blood glucose levels of rats in each group after 4 weeks of ESP administration. ****$P < 0.0001$, ***$P < 0.001$, *$P < 0.05$.

Figure 3. Effects of *Erythropalum scandens* Bl. polysaccharides on blood glucose in rats induced by a high-fat and high-sugar diet combined with potassium oxonate.

4.3. Effects of ESP on Serum Uric Acid Indexes in HUA Rats

Elevated serum uric acid (UA) is the hallmark pathological feature of hyperurice-

mia (HUA) and serves as both a critical diagnostic biomarker and a key metric for assessing therapeutic efficacy. As illustrated in Figure 4, the Control group exhibited a mean serum UA level of 391.2 μmol/L, whereas the HUA model group showed a marked elevation to 1058.3 μmol/L ($P < 0.01$)—representing an approximately 2.7-fold increase. This substantial elevation confirms the successful establishment of the HUA model and demonstrates significant disruption of uric acid metabolism in the model rats.

Following ESP intervention, serum UA levels were significantly reduced compared to the Model group, decreasing to 700.1 μmol/L in the ESP-L group and further to 531.6 μmol/L in the ESP-H group ($P < 0.05$). Notably, the uric acid-lowering effect in the ESP-H group was significantly superior to that observed in the ESP-L group. This dose-dependent response substantiates the role of ESP in modulating uric acid metabolism in HUA rats, providing compelling experimental evidence for non-pharmacological interventions in hyperuricemia management.

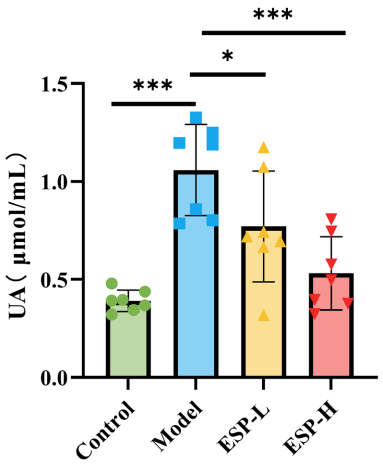

Note: Figure 4 shows serum UA levels in rats of each experimental group. ***$P < 0.001$, **$P < 0.01$, *$P < 0.05$.

Figure 4. Effects of ESP on serum uric acid (UA) in HUA rats.

4.4. Effects of ESP on Histomorphology of Liver, Pancreas and Kidney Tissues in HUA Rats

4.4.1. Liver

HE staining results of liver tissues are shown in Figure 5(A). In the Control group, hepatic lobule architecture remained intact, with hepatocytes displaying their characteristic polygonal shape and arranged in an orderly radial pattern; cells showed abundant cytoplasm and portal vein structures were clearly visible. By contrast, the Model group exhibited extensive fatty and granular degeneration throughout the hepatocytes, with fatty degeneration covering 16.4% ± 0.66% of the area; cell arrangement was highly disordered, indicating severe hepatocyte injury. In the ESP-L group, both fatty and granular degeneration were markedly reduced, and the previously disordered hepatocyte arrangement showed initial

signs of improvement. The ESP-H group demonstrated even more pronounced benefits: fatty degeneration dropped to just 2.3% ± 0.21%, with hepatocyte arrangement and morphology approaching normal levels.

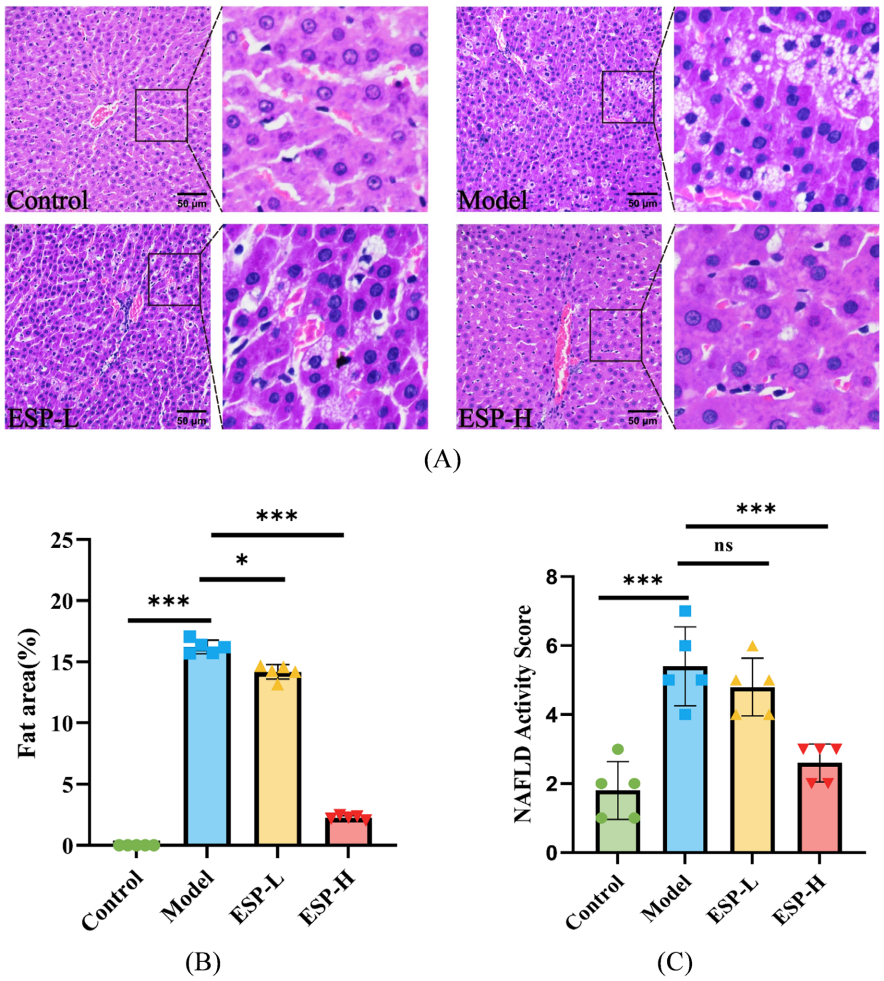

Note: Panel A shows HE staining images of rat liver tissues in each experimental group; Panel B shows the percentage of fatty area; Panel C shows NAFLD activity score. Scale bar = 50 μm.

Figure 5. Representative photomicrographs of rat liver tissue sections (×400).

4.4.2. Pancreas

HE staining results of pancreatic tissues are shown in Figure 6; in the Control group, islet architecture remained intact (black arrows), with abundant β-cells and well-defined acinar cells (red arrows) showing plentiful cytoplasm. The Model group, however, presented a starkly different picture: islets were markedly reduced in number or completely absent (black arrows), β-cell counts dropped sharply, extensive acinar cell necrosis occurred with disorganized arrangement (red arrows), and islet cytoplasm showed clear degenerative changes. Both ESP-L and ESP-H groups demonstrated substantial recovery—islet and β-cell numbers increased significantly, acinar cell necrosis was markedly reduced, and overall pan-

creatic tissue damage showed remarkable improvement compared to the Model group.

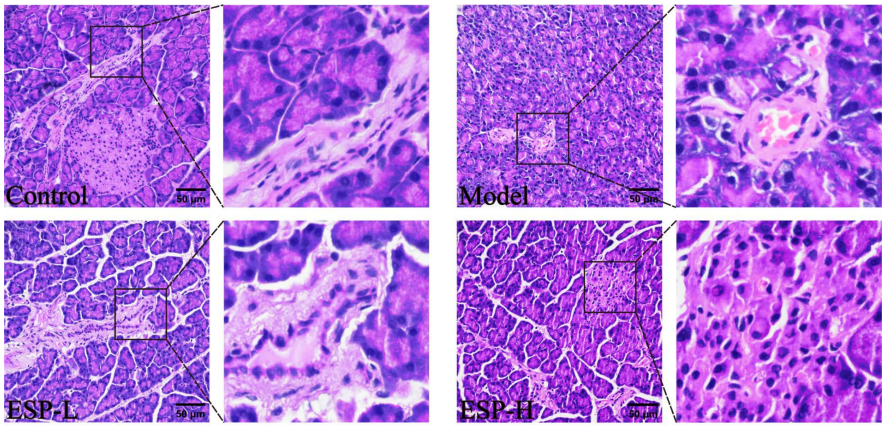

Note: Panel 6 shows HE staining images of pancreatic tissues in rats of each experimental group; Scale bar = 50 μm.

Figure 6. Representative photomicrographs of rat islet tissue sections (×400).

4.4.3. Kidney

HE staining results of kidney tissues are shown in **Figure 7**; in the Control group, glomerular and tubular structures appeared clear and intact, with regular capsular spaces and well-defined boundaries. The Model group showed considerable damage: glomeruli displayed obvious atrophy, tubular epithelial cells underwent necrosis, and various pathological injuries including fatty degeneration were evident. The ESP-L group showed partial improvement—fatty degeneration and epithelial cell necrosis in the tubules were reduced, though glomerular structure remained incompletely restored. In the ESP-H group, recovery was nearly complete: glomerular architecture was essentially returned to normal, fatty degeneration and epithelial cell necrosis were markedly improved, and overall kidney tissue morphology approached healthy levels.

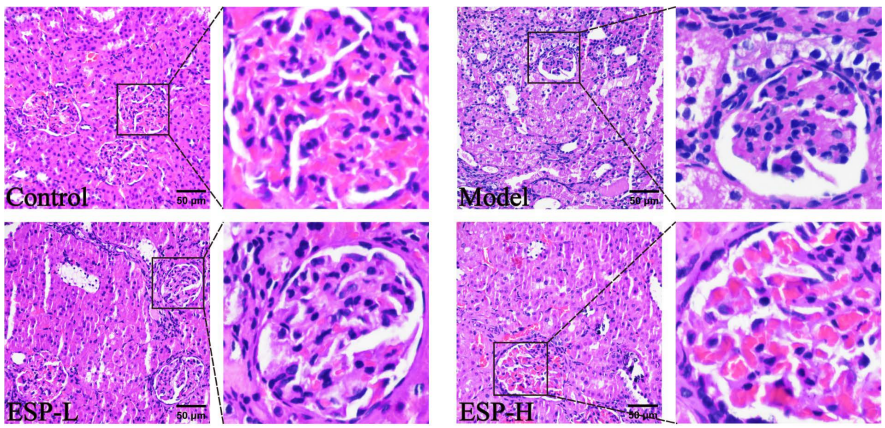

Note: Panel 7 shows HE staining images of kidney tissues in rats of each experimental group; Scale bar = 50 μm.

Figure 7. Representative photomicrographs of rat kidney tissue sections (×400).

5. Discussion

Hyperuricemia (HUA) is frequently comorbid with glucose metabolism disorders, and both represent core components of metabolic syndrome that impose a substantial burden on global public health [7]-[9]. Epidemiological evidence has demonstrated that long-term high fructose intake and a high-fat diet are key environmental triggers for HUA complicated by diabetes [10] [11], and excessive fructose consumption not only elevates the risk of HUA development but also induces glucose-lipid metabolic disorders [12] [13]. Natural medicinal agents have garnered considerable attention for the comprehensive management of metabolic diseases owing to their inherent advantages, including multi-component composition, multi-targeted activity, and low toxic side effects [14] [15]. In the present study, *Erythropalum scandens* Bl. polysaccharide (ESP) was employed as the interventional agent; we systematically evaluated its therapeutic effects in a fructose-induced rat model of HUA with glucose metabolism disorders while optimizing the ESP extraction process. This work is intended to provide experimental evidence to support the development and clinical application of ESP in the treatment of metabolic diseases.

In the present study, we established a rat model of hyperuricemia (HUA) complicated by glucose metabolism disorders using a high-sugar, high-fat diet in combination with potassium oxonate (OXO). This model accurately recapitulates the "four highs" (hyperuricemia, hyperglycemia, hyperlipidemia, and obesity) characteristic of human metabolic syndrome, thereby serving as an ideal tool for investigating disease pathogenesis and evaluating drug interventions, as well as providing theoretical support for clinical prevention and treatment.

As a specific inhibitor of uricase, OXO blocks the uric acid catabolic pathway, impairs renal tubular function, and reduces uric acid excretion. When used alone, it only induces a stable HUA model without causing significant glucose-lipid metabolic disorders [16] [17]. Following intestinal absorption, a high-fructose diet accelerates purine catabolism and promotes uric acid production [18]-[20]; it also interferes with the insulin signaling pathway, drives de novo hepatic lipogenesis, and elicits glucose-lipid imbalance [6]. Additionally, a high-fat diet exacerbates insulin resistance through the accumulation of free fatty acids, induces lipid metabolic disorders and chronic low-grade inflammation, and further amplifies metabolic abnormalities [21].

Regarding the optimization of the ESP extraction process, we employed the hot water extraction-ethanol precipitation method and identified the optimal parameters as follows: a material-to-liquid ratio of 1:20 (g:mL), an extraction temperature of 80˚C, and two extraction cycles of 1 hour each. Under these optimized conditions, the polysaccharide content reached 51.73%, with both extraction efficiency and purity meeting the requirements for subsequent animal experiments. In terms of regulating glucose and uric acid metabolism, ESP exhibited significant dual-improving effects. Animal experimental results demonstrated that serum uric acid (UA) and fasting blood glucose (FBG) levels were significantly elevated

in the model group, indicating successful model establishment and the presence of typical dual disorders of glucose and purine metabolism in the rats. Following 4 weeks of ESP intervention, serum UA and FBG levels decreased in a dose-dependent manner, with the ESP-H group (17.7 mg/mL) exerting the most pronounced therapeutic effect. This finding suggests that ESP possesses prominent uric acid-lowering and blood glucose-lowering activities, as it can regulate uric acid production, excretion, and glucose homeostasis, thereby exerting favorable intervention effects on HUA complicated by glucose metabolism disorders. This observation is consistent with the multi-target regulatory advantage inherent to natural medicines.

ESP also exhibited distinct antioxidant, anti-inflammatory, and organ-protective effects. In the context of HUA complicated by glucose metabolism disorders, reactive oxygen species (ROS) induced by hyperuricemia and hyperglycemia impair antioxidant enzyme activity, promote the accumulation of oxidative products, activate inflammatory pathways, and cause damage to multiple organs, including the liver, kidneys, and pancreas [3]. Histopathological findings revealed obvious hepatic steatosis, renal glomerular atrophy, renal tubular injury, pancreatic islet dysfunction, and a reduction in β-cell number in the model group. In contrast, ESP intervention reduced lipid droplet deposition in the liver, improved nephron integrity, and ameliorated pancreatic islet morphology. These results confirm that ESP alleviates metabolic disorder-induced pathological damage by protecting key metabolic organs. Previous studies have demonstrated that other plant polysaccharides exert metabolic regulatory effects by inhibiting xanthine oxidase (XOD) activity, upregulating the expression of uric acid transporters (URAT1 and GLUT9), improving insulin signaling pathways, and reducing oxidative stress and inflammation [22] [23].

The core finding of the present study is that ESP exerts comprehensive interventional and organ-protective effects in rats with HUA complicated by glucose metabolism disorders. Specifically, it can simultaneously improve uric acid and blood glucose levels and repair multi-organ pathological damage—making it more aligned with the demands of comprehensive metabolic disease treatment than single-target clinical agents. Notably, the ESP-H group exhibited a significantly superior interventional effect compared to the ESP-L group, indicating that the efficacy of ESP is dose-dependent. Future studies involving gradient dose experiments should further optimize the administration dose to achieve the optimal therapeutic outcome. This study also has certain limitations. First, the core active components of ESP that underpin its uric acid-lowering, blood glucose-lowering, and organ-protective effects remain unclear. Second, we only investigated the overall effects of crude ESP polysaccharides, without performing ESP purification, fractionation, structural analysis, or molecular-level detection of relevant transporters, signaling molecules, and inflammatory factors. To address these limitations, future research should optimize the ESP purification process, isolate and identify its core active components, and reveal the underlying regulatory pathways using techniques

such as qPCR, Western blot, and network pharmacology. Additionally, long-term safety and dose-effect relationship evaluations should be conducted to provide precise theoretical and clinical support for the clinical translation of ESP.

Acknowledgements

This work was supported by the National Natural Science Foundation of China (No. 31860094), the Natural Science Foundation of Guangxi (No. 2025GXNSFHA069101).

Conflicts of Interest

The authors declare that there are no conflicts of interest regarding the publication of this paper.

References

[1] Lubawy, M. and Formanowicz, D. (2023) High-Fructose Diet-Induced Hyperuricemia Accompanying Metabolic Syndrome-Mechanisms and Dietary Therapy Proposals. *International Journal of Environmental Research and Public Health*, **20**, Article No. 3596. https://doi.org/10.3390/ijerph20043596

[2] Patodkar, H. and Mohan, M. (2022) A Review on Effects of High Fructose Diet on Oxidative Stress and Metabolic Syndrome in Male Wistar Rats. *International Journal of Pharmaceutical Sciences Review and Research*, **74**, 46-50. https://doi.org/10.47583/ijpsrr.2022.v74i01.008

[3] Vareldzis, R., Perez, A. and Reisin, E. (2024) Hyperuricemia: An Intriguing Connection to Metabolic Syndrome, Diabetes, Kidney Disease, and Hypertension. *Current Hypertension Reports*, **26**, 237-245. https://doi.org/10.1007/s11906-024-01295-3

[4] Baharuddin, B. (2024) The Impact of Fructose Consumption on Human Health: Effects on Obesity, Hyperglycemia, Diabetes, Uric Acid, and Oxidative Stress with a Focus on the Liver. *Cureus*, **16**, e70095. https://doi.org/10.7759/cureus.70095

[5] Agarwal, V., Das, S., Kapoor, N., Prusty, B. and Das, B. (2024) Dietary Fructose: A Literature Review of Current Evidence and Implications on Metabolic Health. *Cureus*, **16**, e74143. https://doi.org/10.7759/cureus.74143

[6] Helsley, R.N., Moreau, F., Gupta, M.K., Radulescu, A., DeBosch, B. and Softic, S. (2020) Tissue-Specific Fructose Metabolism in Obesity and Diabetes. *Current Diabetes Reports*, **20**, Article No. 64. https://doi.org/10.1007/s11892-020-01342-8

[7] Yang, T., Luo, L., Luo, X. and Liu, X. (2025) Metabolic Crosstalk and Therapeutic Interplay between Diabetes and Hyperuricemia. *Diabetes Research and Clinical Practice*, **224**, Article ID: 112204. https://doi.org/10.1016/j.diabres.2025.112204

[8] Singh, S.K., Singh, R., Singh, S.K., Iquebal, M.A., Jaiswal, S. and Rai, P.K. (2023) Uric Acid and Diabetes Mellitus: An Update. *Postgraduate Medical Journal*, **99**, 1220-1225. https://doi.org/10.1093/postmj/qgad081

[9] Zhang, C., Li, L., Zhang, Y. and Zeng, C. (2020) Recent Advances in Fructose Intake and Risk of Hyperuricemia. *Biomedicine & Pharmacotherapy*, **131**, Article ID: 110795. https://doi.org/10.1016/j.biopha.2020.110795

[10] He, L., Miao, M., Li, Q., Cheng, J. and Li, R. (2025) Evaluation of the Effects of High Uric Acid on Glucolipid Metabolism, Renal Injury and the Gut Microbiota in Diabetic Male Hamsters with Dyslipidemia. *Toxics*, **13**, Article No. 751. https://doi.org/10.3390/toxics13090751

[11] Lin, Z. and Sun, L. (2024) Research Advances in the Therapy of Metabolic Syndrome. *Frontiers in Pharmacology*, **15**, Article ID: 1364881. https://doi.org/10.3389/fphar.2024.1364881

[12] Tero-Vescan, A., Ştefănescu, R., Istrate, T. and Puşcaş, A. (2024) Fructose-Induced Hyperuricaemia—Protection Factor or Oxidative Stress Promoter? *Natural Product Research*, **39**, 948-960. https://doi.org/10.1080/14786419.2024.2327624

[13] Liu, Y., Han, F., Ma, X., Yang, L. and Shi, Z. (2025) Organic Acids from Ice Wine Ameliorate Fructose-Induced Disorders of Glycolipid Metabolism in C57BL/6J Mice. *Food & Function*, **16**, 3296-3307. https://doi.org/10.1039/d4fo05580b

[14] Shen, X., Yang, H., Yang, Y., Zhu, X. and Sun, Q. (2024) The Cellular and Molecular Targets of Natural Products against Metabolic Disorders: A Translational Approach to Reach the Bedside. *MedComm*, **5**, e664. https://doi.org/10.1002/mco2.664

[15] Tabatabaei-Malazy, O., Lavari, N. and Abdollahi, M. (2024) Natural Products in the Clinical Management of Metabolic Syndrome. In: Wainwright, C.L. and Schini-Kerth, V.B., Eds., *Handbook of Experimental Pharmacology*, Springer, 123-157. https://doi.org/10.1007/164_2024_711

[16] Chau, Y., Chen, H., Lin, P. and Hsia, S. (2019) Preventive Effects of Fucoidan and Fucoxanthin on Hyperuricemic Rats Induced by Potassium Oxonate. *Marine Drugs*, **17**, Article No. 343. https://doi.org/10.3390/md17060343

[17] Xu, Z., Sha, W., Hou, C., Amakye, W.K., Yao, M. and Ren, J. (2022) Comparison of 3 Hyperuricemia Mouse Models and Evaluation of Food-Derived Anti-Hyperuricemia Compound with Spontaneous Hyperuricemia Mouse Model. *Biochemical and Biophysical Research Communications*, **630**, 41-49. https://doi.org/10.1016/j.bbrc.2022.09.043

[18] Wen, S., Arakawa, H. and Tamai, I. (2024) Uric Acid in Health and Disease: From Physiological Functions to Pathogenic Mechanisms. *Pharmacology & Therapeutics*, **256**, Article ID: 108615. https://doi.org/10.1016/j.pharmthera.2024.108615

[19] Brouns, F. (2020) Saccharide Characteristics and Their Potential Health Effects in Perspective. *Frontiers in Nutrition*, **7**, Article No. 75. https://doi.org/10.3389/fnut.2020.00075

[20] Dziadek, K., Kopeć, A., Piątkowska, E. and Leszczyńska, T. (2019) High-Fructose Diet-Induced Metabolic Disorders Were Counteracted by the Intake of Fruit and Leaves of Sweet Cherry in Wistar Rats. *Nutrients*, **11**, Article No. 2638. https://doi.org/10.3390/nu11112638

[21] Hernández-Díazcouder, A., Romero-Nava, R., Carbó, R., Sánchez-Lozada, L.G. and Sánchez-Muñoz, F. (2019) High Fructose Intake and Adipogenesis. *International Journal of Molecular Sciences*, **20**, Article No. 2787. https://doi.org/10.3390/ijms20112787

[22] Ullah, Z., Yan, Z., Zhang, M., Liu, P., Yue, P., Zhao, T., *et al*. (2025) A Comprehensive Review on Targeting Hyperuricemia with Edible Bioactive Polysaccharides: Advances in Structure, Xanthine Oxidase Inhibition, Uric Acid-Lowering Strategies, Mechanisms, and Current Applications. *Food Reviews International*, 1-39. https://doi.org/10.1080/87559129.2025.2513014

[23] Arunachalam, K., Sreeja, P.S. and Yang, X. (2022) The Antioxidant Properties of Mushroom Polysaccharides Can Potentially Mitigate Oxidative Stress, Beta-Cell Dysfunction and Insulin Resistance. *Frontiers in Pharmacology*, **13**, Article ID: 874474. https://doi.org/10.3389/fphar.2022.874474